ISSN 1990-7931, Russian Journal of Physical Chemistry B, 2020, Vol. 14, No. 4, pp. 642–646. © Pleiades Publishing, Ltd., 2020.
Russian Text © The Author(s), 2020, published in Khimicheskaya Fizika, 2020, Vol. 39, No. 8, pp. 46–50.

COMBUSTION, EXPLOSION, AND SHOCK WAVES

Attenuation of Shock Waves in Reactive Materials

A. Yu. Dolgoborodov[a, b, c, *]

[a]*Joint Institute for High Temperatures, Russian Academy of Sciences, Moscow, 125412 Russia*
[b]*Semenov Federal Research Center for Chemical Physics, Russian Academy of Sciences, Moscow, 119991 Russia*
[c]*National Research Nuclear University MEPhI (Moscow Engineering Physics Institute), Moscow, 115409 Russia*
**e-mail: aldol@ihed.ras.ru*

Received January 15, 2020; revised January 15, 2020; accepted February 20, 2020

Abstract—The results of an experimental study of shock wave (SW) attenuation in mixtures of magnesium and aluminum with solid metal oxides upon contact blasting of explosive charges are presented. Faster attenuation is found in reactive mixtures compared to homogeneous materials of similar compressibility and inert mixtures, which is related to the occurrence of fast reactions of components behind the SW front with an increase in the density and, correspondingly, unloading wave velocities.

Keywords: shock wave, attenuation, termite mixtures
DOI: 10.1134/S1990793120040144

INTRODUCTION

Detonation of condensed explosives (CEs) leads to the formation in the environment of shock waves (SWs) that cause irreversible destruction. Protective structures made of various materials are used for protection against the effects of SWs and explosion products. To determine the effectiveness of the use of certain materials, information is needed on their behavior under shock loading concerning the laws of SW attenuation in homogeneous, porous, or composite materials of a different compressibility and structure. Various methods of attenuation of SWs at a considerable distance from explosive charges have been studied in detail (see, for example, [1, 2]). As for the attenuation of SWs in the near zone during a contact explosion, in most experimental studies of attenuation, various experimental settings, which were determined by the specific conditions for the use of certain devices, were used. The use of such data to obtain general regularities is rather difficult, since quite often in experiments there is non-dimensional loading or interaction with side rarefaction waves [3, 4]. The results of studying the attenuation of plane SWs under conditions of one-dimensional loading using explosive charges or plate impact are presented in a number of works (see, for example, [5–7]); however, the data were obtained mainly for solid materials (metals, rocks, and some plastics) without taking into account the possible physical and chemical transformations of substances behind the front of the SW.

During the shock compression of a number of substances and mixtures, various physical and chemical transformations can occur in them, accompanied by effects that are useful in terms of the attenuation of the SW's amplitude. Since the attenuation of strong SWs at the time scales characteristic of a contact explosion of the explosive charge occurs mainly due to unloading in the back and side rarefaction waves, the types of transformations that lead to an abnormal increase in the density of the medium behind the shock front are of interest. Such types of transformations lead to an increase in the velocity of rarefaction waves in such materials and, consequently, to an increase in the attenuation of SWs in comparison with other materials. Earlier, we studied the efficiency of the attenuation of plane SWs in organic, porous, and composite materials with a change in the density and content of the fillers and binders [8–11]. It was shown that in the case of polymorphic transformations in substances with a decrease in the specific volume behind the SW front, it is possible to obtain higher attenuation coefficients compared to substances without transformations. This paper presents the results of a study of the attenuation of plane SWs in samples of thermite mixtures based on magnesium powders with titanium, silicon, and iron oxides (TiO_2, SiO_2, Fe_2O_3), as well as aluminum powder with Fe_2O_3, which react with the formation of products with a lower specific volume than the initial material.

EXPERIMENTAL

In the experiments, attenuation of plane SWs with a triangular pressure profile with the increasing thickness of the samples was studied. Shock waves were created upon the contact detonation of explosive charges.

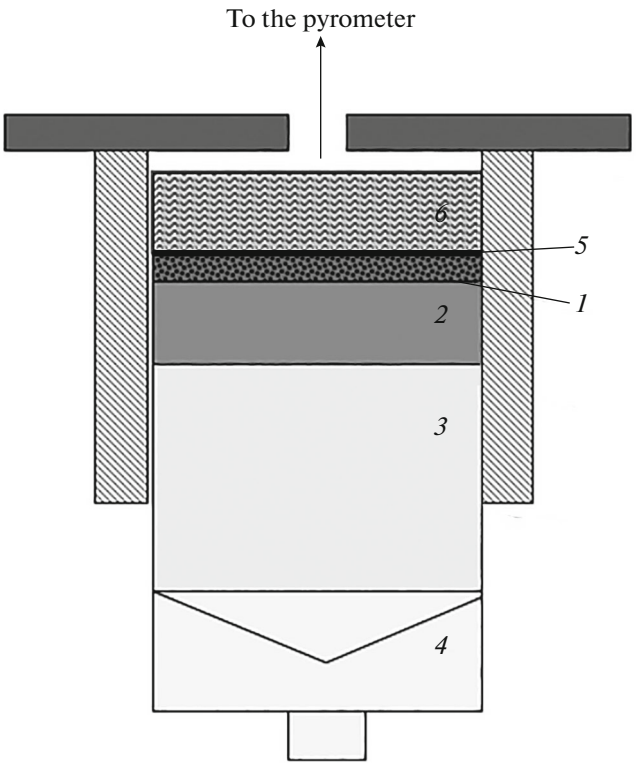

Fig. 1. Setting the experiments to determine the attenuation of plane SWs in various samples: (*1*) sample; (*2*) octogen charge; (*3*) TNT charge; (*4*) lens; (*5*) aluminum foil; (*6*) indicator.

The mixtures were prepared by the mechanical mixing of powders of Mg of the MPF-1 (milled irregular particles with the average size of about 310 μm) and MPF-3 (130 μm) brands, Al powder of the ASD-1 brand (50 μm), and powders of chemically pure TiO_2, SiO_2, and Fe_2O_3 oxides. The average particle size of the oxidizing agents was 10–20 μm. Samples with a diameter of 40 mm and a thickness of 1 to 10 mm were made by cold pressing.

The experiments were carried out according to a scheme similar to the one used previously [10] (Fig. 1). The SW in the sample was created upon detonation of the charge of a powerful CE (PCE) of a hexogen (density 1.71 g/cm^3) or octogen (1.80 g/cm^3) with a diameter of 40 mm and a height of 10 mm. To initiate the PCE, a charge of trinitrotoluene (TNT) with a reduced density of 1.35 g/cm^3 and a height of 50 mm was used, which in turn was initiated by a plane front generator (a lens made from a TNT/RDX mixture). The duration for which the increased parameters in a shock-compressed sample are retained is determined by the height of the charge of the PCE. The decay of the parameters behind the detonation wave front in the PCE charge outside the lateral expansion zone is determined by the centered rarefaction wave from the contact boundary between the PCE and TNT charges until the states related to the TNT charge's detonation parameters are reached. The temporal profile of the mass velocity behind the wave front is close to triangular, and the characteristic lengths of the region of the centered rarefaction wave at the end of the PCE charge are about 1 mm. Such a setting of the experiments made it possible to create plane SWs in the studied media that effectively attenuated at a thickness of several mm and to exclude the influence of side unloading waves at the initial stage of attenuation with a duration of up to 2–3 μs, which allowed us to compare the obtained attenuation data with the simple one-dimensional calculations.

The value of the pressure transmitted through the samples was measured by the indicator method [12] using bromoform $CHBr_3$ or carbon tetrachloride CCl_4. Aluminum foil with a thickness of 20 μm was placed between the samples and the indicator. The use of a liquid indicator makes it possible to exclude the influence of loading inhomogeneity at the contact boundary with a porous sample, which occurs when pressure sensors are used due to their destruction at the boundary with a porous sample. The glow of the front of the SW in the indicator liquid was recorded by an electron-optical pyrometer through a 5 mm diameter diaphragm located in the central part of the sample and was converted to the brightness temperature T. The pressure value P at the SW front in the indicator was determined from the known dependences [12]: $T = 237 + 112\,P$ for $CHBr_3$ and $T = 343 + 121\,P$ for CCl_4, where T is in K and P is in GPa. The temporal resolution of recording the radiation was 20 ns and the accuracy of determining the pressure was 0.2–0.3 GPa. In a number of experiments, the brightness temperature of the products of the shock-induced chemical reaction was also measured. In this case, instead of an indicator, a lithium fluoride (LiF) window was placed on the contact boundary of the sample without foil, which retained the transparency under shock compression in the pressure range under consideration.

RESULTS AND DISCUSSION

The experimental pressure drop curves in the indicator with increasing sample thickness x were approximated by the exponential dependence of the pressure on the sample thickness: $P(x) = P_0\exp(-\alpha x)$, with the minimization of the deviations by the least squares method, where P_0 was the pressure at zero sample thickness and α was the attenuation coefficient. The value of P_0 was determined in experiments with samples of the minimum thickness (less than 2 mm) at a charge height of the RDX or HMX of 50 mm. The form of the dependence $P(x)$ is determined by traditional considerations about the exponential nature of the attenuation, and, in addition, the experimental data are described by the exponential dependence with the highest correlation coefficient within the pressure

drop in the indicator to $P = 0.5P_0$. The experimental data processing for various mixtures are presented in Table 1. This table shows the type of metal powder; the weight composition of the mixture; ρ_0, the density of the samples; ε, the porosity; α, the attenuation coefficient with the thickness of the samples; α_m, the attenuation coefficient per specific mass; the asterisks denote the data were obtained with the $CHBr_3$ indicator; the rest of the data were obtained with CCl_4. For comparison, the data are also presented here for mixtures of inert Al components with polymethyl methacrylate (PMMA) and potassium iodide KI, as well as for porous Al.

It should be noted that there is a qualitative difference in the nature of the increase in pressure profiles in the indicator for mixtures of inert and reactive components. Figure 2 illustrates examples of recording pressure profiles in $CHBr_3$ that were transferred through a 1.7-mm-thick sample of a reactive $Mg(MPF\text{-}1)/TiO_2$ mixture from a 10-mm-thick RDX charge and an inert Al(ACD-1)/KI mixture sample 1.5 mm thick from an RDX charge 50 mm thick. In the case of loading samples during the detonation of an elongated charge, a sharp increase in pressure (less than 20 ns) was observed for inert mixtures, followed by a monotonic decrease (Fig. 2, curve *2*), and in the case of reacting of Mg mixtures, profiles with a time-delayed (about 0.21 μs) increase in pressure were obtained (Fig. 2, curve *1*). For the Al/Fe_2O_3 mixture, the pressure increase is less pronounced (50–100 ns).

Since the pressure profiles in the experiments with long and short charges differed in the character of the rise and fall, which could be related to the features of the reaction during a rapid drop in pressure in the case of short charges, the data were also processed for a number of mixtures without taking into account the P_0 values, obtained in experiments with long charges. These values are given in Table 1 in brackets.

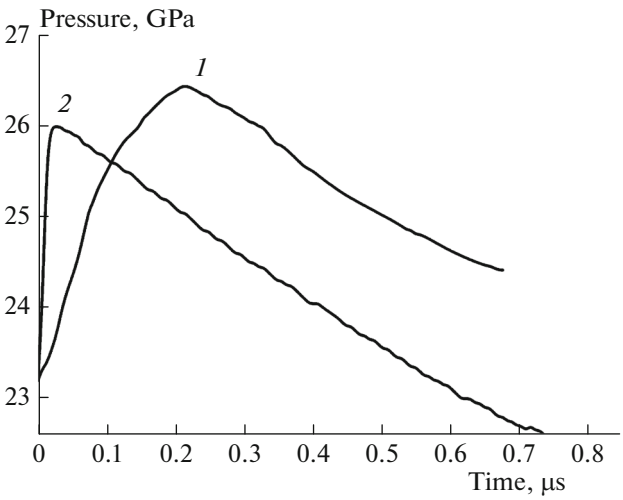

Fig. 2. Pressure profiles in the indicator ($CHBr_3$) located after the samples of the termite mixture Mg/TiO_2 (*1*) and the mixture of inert components Al/KI (*2*).

The reasons for the increase in the attenuation coefficients in the reacting mixtures and inert samples were analyzed. If the assumption that—in the case of a plane SW, the attenuation mainly occurs due to the

Table 1. Experimental data on SW attenuation in mixtures

Mixture	Weight composition	ρ_0, g/cm^3	ε, %	P_0, GPa	α, 10^{-1} mm^{-1}
$Mg(MPF\text{-}3)/SiO_2$	40/60	1.01	50	28.8*	1.71 ± 0.27
$Mg(MPF\text{-}1)/SiO_2$	40/60	1.28	40	32.5* (24.0)	1.56 ± 0.38 (0.93)
$Mg(MPF\text{-}3)/TiO_2$	32/68	2.05	30	31.2*	1.43 ± 0.39
$Mg(MPF\text{-}1)/TiO_2$	32/68	2.05	30	33.5* (29.6)	1.39 ± 0.20 (0.72)
$Mg(MPF\text{-}3)/Fe_2O_3$	69/31	1.96	10	23.4 (20.4)	1.01 ± 0.18 (0.72)
$Mg(MPF\text{-}1)/Fe_2O_3$	31/69	2.32	28	23.6 (18.9)	1.47 ± 0.34 (0.92)
$Al(ASD\text{-}1)/Fe_2O_3$	35/65	2.79	30	22.8 (17.1)	1.40 ± 0.43 (0.70)
Al(ASD-1)/ PMMA	50/50	1.15	30	22.7	0.82 ± 0.16
Al(ASD-1)/KI	50/50	2.02	30	20.6	0.86 ± 0.13
				26.0*	0.85 ± 0.25
Al(ASD-1)	100	1.89	30	21.4	0.83 ± 0.10

* The asterisks denote the data were obtained with the $CHBr_3$ indicator; the rest of the data were obtained with CCl_4.

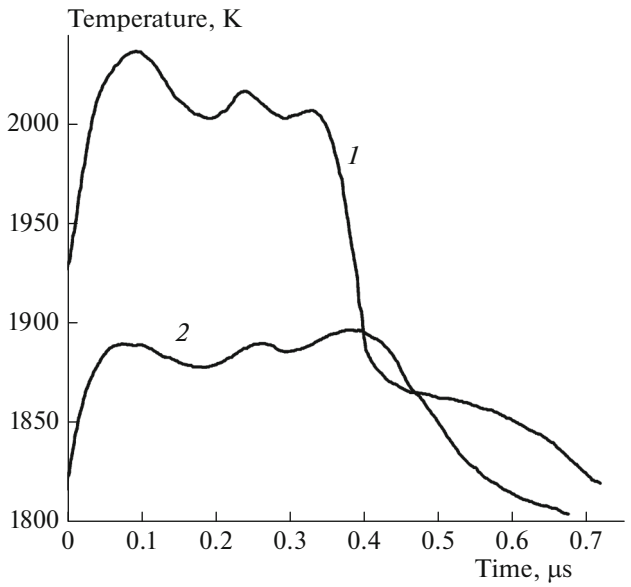

Fig. 3. The brightness temperature profiles (λ = 627 nm) at the contact boundary with LiF for mixtures of Mg(MPF-3)/TiO_2 (*1*) and Mg(MPF-3)/Fe_2O_3 (*2*).

rarefaction waves catching up [8]—is true, then the ratio $C/(C + u - D)$ is decisive for the rate of attenuation, where C is the speed of sound behind the wave front, u is the mass velocity, and D is the velocity of the SW. The shock adiabats calculated on the assumption of additivity of the specific volumes of the components of the nonreacting mixtures of magnesium with titanium oxides at their mass ratio of 32/68 and the mass ratio of iron of 31/69 at pressures of 20 to 40 GPa in the diagrams have the pressure–mass velocity behind the front close to that of the shock adiabat of aluminum. However, the SW attenuation in mixtures is much faster than in pure aluminum. The most probable reason for the faster SW attenuation in mixtures of magnesium and aluminum with oxides is the occurrence of chemical reactions behind the wave fronts with a significant decrease in the specific volume, the consequence of which would be a significant decrease in the velocity of propagation of wave D and an increase in the mass velocity u behind the front at equal pressures. The reactions of the components of the mixtures proceed with the formation of denser products compared to the initial mixtures: $2Mg + TiO_2 \rightarrow 2MgO + Ti$; $2Mg + SiO_2 \rightarrow 2MgO + Si$; $3Mg + Fe_2O_3 \rightarrow 3MgO + 2Fe$; and $2Al + Fe_2O_3 \rightarrow Al_2O_3 + 2Fe$. With a stoichiometric ratio of the components, the densities of the starting mixtures under normal conditions are 2.75, 2.13, 3.20, and 4.25 g/cm^3; and for the reaction products, 3.97, 3.25, 4.95, and 5.42 g/cm^3, respectively. Thermal heating as a result of the reaction, the different compressibility of the components, and the polymorphic transitions in titanium and silicon at high pressures slightly change these differences quantitatively; however, the additional decrease in the specific volume behind the wave front is maintained.

Based on the data obtained, it is impossible to estimate the depth of the reaction during the time of the shock compression; however, the temperature measurement results are additional confirmation of the presence of noticeable chemical transformations behind the shock fronts in the mixtures under consideration. In the experiments, the optical windows of LiF were placed instead of the indicator at the contact boundary of the samples. The shock adiabat of LiF in the P–u coordinates does not differ much from the calculated shock adiabats of the mixtures; therefore, it can be assumed that the recorded temperatures are close to the temperatures behind the shock front in the mixtures. The shock waves in these experiments were created upon the impact of a plate of duralumin, previously accelerated by the products of the explosion. The waves' intensities were approximately the same as in the experiments with the elongated RDX charges. The brightness temperatures of the contact boundaries for the Mg/Fe_2O_3 and Mg/TiO_2 mixtures at the sample porosity of about 10% were, respectively, about 1900 and more than 2000 K at pressures in the transmitted wave of 27 and 26 GPa. These values are significantly higher than those that can be obtained in the calculations for nonreacting mixtures. Examples of the recording profiles of the brightness temperature at the wavelength of λ = 627 nm are shown in Fig. 3.

In addition to the chemical reaction with the formation of denser products, high sample porosity also affects on high attenuation coefficients in termite mixtures. It is possible that the rapid attenuation of waves in porous samples is related to the faster reaction during collapse of the pores and mixing of the components during the compression of the porous mixtures. From this point of view, we should expect a slower attenuation of the waves in low-porous samples of mixtures, and their use to attenuate SWs under specific conditions should be accompanied by the appropriate experimental verification.

The course of a chemical transformation under shock compression is generally determined not only by the SW parameters at the front but also by the kinetics of the course of this transformation and, accordingly, depends on the change in pressure with time, which is determined by the charge height in front of the sample or the thickness of the impact plate. At similar values of the decay time of the parameters and the transformation time, the conversion rate realized in the process and the degree of conversion achieved can be expected to be lower with shorter times of the pressure drop behind the wave front. For this reason, the experimental results with the same ratio of the sample and charge size but with a different real size can qualitatively differ, although for nonreacting media they would be similar. It is possible that this is one of the reasons for the difference in the attenuation coeffi-

cients obtained by processing data with only short charges and taking into account the data for long charges. A quantitative consideration of these features requires special studies of the kinetics of the reaction during the shock compression of thermite mixtures, taking into account the real structure of the samples.

CONCLUSIONS

The result of the experimental study of the attenuation of SWs formed by the contact explosion of RDX and HMX charges in thermite mixtures of magnesium powders with titanium, silicon and iron oxides, as well as aluminum powder with iron oxide, showed an increase in the SW attenuation coefficients in these mixtures compared to mixtures of nonreacting components. The elevated brightness temperatures (at the level of 2000 K) of shock-compressed mixtures at the contact boundary with a transparent window made of LiF were also recorded, which is evidence of the occurrence of shock-induced reactions in the mixtures. The increase in the attenuation rate can be explained by the decrease in the specific volume of the reaction products compared with the initial mixture, which leads to an increase in the velocities of the rarefaction waves behind the shock front in the denser substance.

REFERENCES

1. B. E. Gel'fand and M. V. Sil'nikov, *Barothermic Action of Explosions* (Asterion, St. Petersburg, 2006) [in Russian].
2. O. Igra, J. Falcovitz, L. Houas, and G. Jourdan, Prog. Aerospace Sci. **58**, 1 (2013).
3. M. Kroh and D. Ludwig, AIP Conf. Proc. **78**, 486 (1982).
4. L. Y. Chi, Z.-X. Zhang, A. Aalberg, J. Yang, and C. C. Li, Int. J. Impact Eng. **125**, 27 (2019).
5. V. N. Kondrat'ev, I. V. Nemchinov, and B. D. Khristoforov, Zh. Prikl. Mekh. Tekh. Fiz., No. 4, 61 (1968).
6. S. Nakazawa, S. Watanabe, Y. Iijima, and M. Kato, Icarus **156**, 539 (2002).
7. M. J. Murphy, M. A. Lieber, and M. M. Biss, AIP Conf. Proc. **1979**, 160020 (2018).
8. I. M. Voskoboinikov, A. Yu. Dolgoborodov, and A. N. Afanasenkov, Fiz. Goreniya Vzryva **19** (5), 135 (1983).
9. I. M. Voskoboinikov and A. Yu. Dolgoborodov, in *Detonation and Shock Waves* (IKhF AN SSSR, Chernogolovka, 1986), p. 9 [in Russian].
10. A. Yu. Dolgoborodov, Khim. Fiz. **17** (5), 102 (1998).
11. M. F. Gogulya, A. Yu. Dolgoborodov, and M. A. Brazhnikov, Int. J. Impact Eng. **23**, 283 (1999).
12. M. F. Gogulya and A. Yu. Dolgoborodov, Khim. Fiz. **13** (12), 118 (1994).

Translated by V. Selikhanovich